Available online at www.sciencedirect.com
SCIENCE DIRECT®
Journal of Crystal Growth 270 (2004) 301–308
JOURNAL OF CRYSTAL GROWTH
www.elsevier.com/locate/jcrysgro

Arsenic cross-contamination in GaSb/InAs superlattices

E.M. Jackson[a,b,*], G.I. Boishin[a,c], E.H. Aifer[a], B.R. Bennett[a], L.J. Whitman[a]

[a]*Naval Research Laboratory, Washington, DC 20375, USA*
[b]*SFA, Inc., Largo, MD 20774, USA*
[c]*NOVA Research Inc., Alexandria, VA 22308, USA*

Received 5 May 2004; accepted 21 June 2004
Communicated by R.S. Feigelson
Available online 27 August 2004

Abstract

We have investigated the cross-contamination of As in GaSb/InAs superlattices. We demonstrate a method of varying the lattice constant of the superlattice. By controlling the As background pressure in the growth chamber, the strain can be controlled to about 0.01%, corresponding to As cross-incorporation variations of about ±1%. The distribution of As is investigated by X-ray diffraction and cross-sectional scanning tunneling microscopy, and the critical thickness is obtained.

PACS: 81.15.Hi; 68.65.Cd; 81.05.Ea

Keywords: A3. Molecular beam epitaxy; A3. Superlattices; B1. Antimonides; B1. Arsenates; B2. Semiconducting III–V materials

1. Introduction

Type II GaSb/InAs superlattices show great promise for long and very–long wavelength infrared detectors. Compared to existing technologies, such as mercury–cadmium–telluride detectors, detectors based on GaSb/InAs superlattices have the potential for lower dark currents due to reduced Auger scattering and a higher electron effective mass. In addition, as a III-V material, their growth and processing is greatly simplified.

One issue that arises in the molecular beam epitaxy (MBE) of these superlattices is cross-contamination of the group V elements [1–3]. In general, it has been treated as a nuisance to be minimized. However,

*Corresponding author. SFA, Naval Research Laboratory, 9315 Largo Drive West, Suite 200, Largo, MD20774, USA. Tel.: +1-2027675458; fax: +1-2024047194.
E-mail address: ejackson@ccf.nrl.navy.mil (E.M. Jackson).

0022-0248/$ - see front matter © 2004 Elsevier B.V. All rights reserved.
doi:10.1016/j.jcrysgro.2004.06.033

Report Documentation Page

Form Approved
OMB No. 0704-0188

1. REPORT DATE	2. REPORT TYPE	3. DATES COVERED
MAY 2004		**00-00-2004 to 00-00-2004**

4. TITLE AND SUBTITLE	5a. CONTRACT NUMBER
Arsenic cross-contamination in GaSb/InAs superlattices	5b. GRANT NUMBER
	5c. PROGRAM ELEMENT NUMBER
6. AUTHOR(S)	5d. PROJECT NUMBER
	5e. TASK NUMBER
	5f. WORK UNIT NUMBER
7. PERFORMING ORGANIZATION NAME(S) AND ADDRESS(ES) **Naval Research Laboratory,4555 Overlook Avenue SW,Washington,DC,20375**	8. PERFORMING ORGANIZATION REPORT NUMBER
9. SPONSORING/MONITORING AGENCY NAME(S) AND ADDRESS(ES)	10. SPONSOR/MONITOR'S ACRONYM(S)
	11. SPONSOR/MONITOR'S REPORT NUMBER(S)

12. DISTRIBUTION/AVAILABILITY STATEMENT
Approved for public release; distribution unlimited

13. SUPPLEMENTARY NOTES

14. ABSTRACT

We have investigated the cross-contamination of As in GaSb/InAs superlattices. We demonstrate a method of varying the lattice constant of the superlattice. By controlling the As background pressure in the growth chamber, the strain can be controlled to about 0:01%, corresponding to As cross-incorporation variations of about +-1%. The distribution of As is investigated by X-ray diffraction and cross-sectional scanning tunneling microscopy, and the critical thickness is obtained.

15. SUBJECT TERMS

16. SECURITY CLASSIFICATION OF:			17. LIMITATION OF ABSTRACT	18. NUMBER OF PAGES	19a. NAME OF RESPONSIBLE PERSON
a. REPORT	b. ABSTRACT	c. THIS PAGE			
unclassified	**unclassified**	**unclassified**	**Same as Report (SAR)**	**8**	

controlled cross-incorporation can be an advantage as it gives device designers another degree of freedom with which to simultaneously optimize the lattice match and other material properties such as the band gap.

Prior studies of cross-contamination have shown that Sb contamination is determined, in part, by the amount of excess Sb in the surface reconstruction during GaSb growth [2], and As cross-contamination is determined by the As background pressure [1,4]. There is, however, always an excess of Sb on the surface associated with the reconstruction under typical Sb-rich growth conditions, so there are limited options for controlling Sb cross-incorporation into InAs [5,6]. By comparison, the As background pressure is comparatively easy to control. The major unknown is the distribution of As at the interfaces within the GaSb layers. Here, we report on a study to determine the distribution of As in GaSb/InAs superlattices.

2. Experimental procedure

A series of 50-period superlattices (SL) with a nominal structure of 40 monolayers (ML) of GaSb on 20 ML of InAs with InSb interfaces were grown by solid source MBE in a Riber 21 T growth chamber. The superlattices were grown at 400 °C at a rate of 1.0 ML/s on (0 0 1) oriented GaSb substrates. InSb interfaces were forced by migration-enhanced epitaxy (MEE). The As and Sb fluxes were produced by valved crackers with tip temperatures of 950 and 900 °C, respectively, producing primarily As_2 and Sb_2. The Sb flux was controlled by a shutter with the Sb valve left open throughout the growth at a setting which produced a flux just sufficient to grow at 2 ML/s. The As flux was controlled by both a valve and a shutter. During InAs growth, the As valve was set to produce a flux sufficient to grow at 2 ML/s with the As shutter open. During GaSb growth the As shutter was closed, and the As valve setting was reduced to a value which was constant during each SL growth, but varied from one SL to the next.

The MEE procedure for forcing InSb interfaces is as follows. At the end of each InAs layer, we reduce the As valve setting, close the shutter, and then deposit 1 ML of In. This is followed by a 2 s Sb soak before beginning GaSb growth. GaSb growth is followed by a 2 s Sb soak. Then the As valve is opened with the shutter closed and 1 ML of In is deposited. The InAs layer is then grown with the As shutter open. A very similar procedure has been shown previously to result in predominantly InSb interfaces [1]. It also ensures that the As pressure is already close to steady state when growth of the GaSb layer begins.

During growth, the background pressure in the chamber was monitored with the growth chamber's flux gauge which was positioned 12.7 cm from the center of the wafer, out of the direct beam fluxes. The measured pressure is a function of the position of the flux gauge. Nevertheless, it will be shown that the background pressure reading (P_b) during the GaSb growth is proportional to the amount of As which incorporates into the GaSb layers.

Cross-sectional scanning tunneling microscopy (XSTM) images were obtained by the procedure described by Nosho et al. [5]. Briefly, to obtain high-quality, atomically flat cleaves, samples were first thinned to $\sim 150\,\mu m$. After loading a sample into the UHV chamber, it was scribed and cleaved along a {1 1 0} plane, exposing a cross-sectional view of the GaSb/InAs SL structure at the cleavage surface. For material with the zinc-blende crystal structure, XSTM images of {1 1 0} surfaces reveal only every other (0 0 1) plane in cross section. The XSTM images shown here were recorded for filled electronic states, typically at 2.4 V and 60 pA, nominally imaging the anion sublattice (i.e. every other row of Sb or As atoms) [7].

High resolution X-ray diffraction (XRD) of the (0 0 4) reflection was performed on the SLs using a Bede QC1 double crystal X-ray diffractometer with a Cu Kα source and a GaSb first crystal. No tilt was detectable. Glancing incidence measurements around the (1 1 5) reflection were also performed to obtain the in-plane lattice constant. In all cases, the in-plane mismatch was less than 5×10^{-4}.

3. Results and discussion

A typical growth log of pressure vs. time is shown in Fig. 1(a). The pressure highs and lows occur during the InAs and GaSb growths, respectively. Even during the GaSb growth, the background pressure is caused almost entirely by As. An approximately steady state is reached within seconds. The pressure is relatively constant during the growth of each layer except for brief transition periods when it is changing from InAs growth to GaSb growth and back [see Fig. 1(b)]. In test runs of the SL growth recipe with the As valve closed, the background pressure was $\sim 1 \times 10^{-8}$ Torr, a factor of 100 less than the low pressure during normal growth. It is well known that the sticking coefficient of Sb and the group III elements on the cold shroud is close to unity. Arsenic builds up in the chamber because it has a much lower sticking coefficient. Since this pressure build-up depends on the design of the chamber and is also position dependent, the values given here are not expected to apply to other growth chambers; however, a similar calibration procedure should be generally applicable.

A typical XRD (0 0 4) rocking curve is shown in Fig. 2. The superlattice period is determined from the spacing of the peaks, and the average c-axis lattice constant of the superlattice is obtained from the position of the 0th order diffraction peak measured relative to the known position of the GaSb substrate diffraction peak. All the SLs in this study were within 3% of the intended period. In Fig. 3, the position of the GaSb (0 0 4) reflection may be compared with the 0th order peak for 3 superlattices with different values of P_b. The 0th order peak shifts toward a higher angle indicating a decreasing lattice constant with increasing P_b. The decreasing lattice constant implies an increasing As concentration in the GaSb layers, since GaAs bonds are $\sim 7\%$ shorter than GaSb bonds.

Using Bragg's law, the z-axis lattice constant c_z can be computed from XRD spectra:

$$c_z = d_{\mathrm{GaSb}} \times \frac{\sin(\theta_{\mathrm{GaSb}})}{\sin(\theta_{\mathrm{GaSb}} + \delta\theta)}, \tag{1}$$

where θ is Bragg's angle for the GaSb (0 0 4) reflection peak, $\delta\theta$ is the position of the 0th order superlattice reflection relative to the substrate peak, and d_{GaSb} is the unstrained GaSb lattice constant. Then the bulk lattice constant, c_{ave}, is determined from c_z assuming Poisson's constant $\approx 1/3$. The results, seen in Fig. 4, show that c_{ave} is a linear function of P_b. The standard deviation from the line is 5×10^{-4},

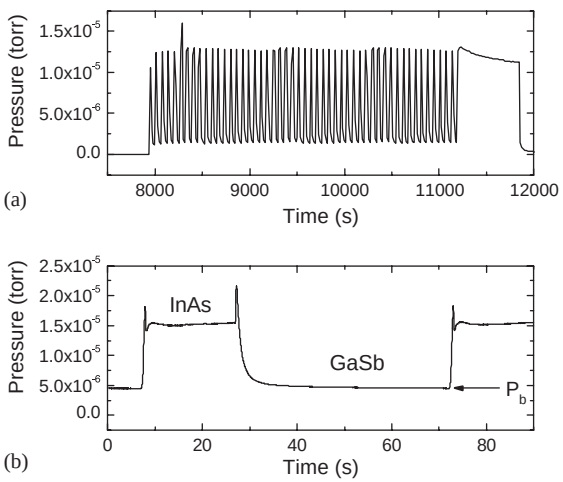

Fig. 1. (a) Pressure reading during superlattice growth for a gauge 12.7 cm away from the wafer. (b) Expanded view of the pressure reading during a single period (of a different growth). P_b is indicated.

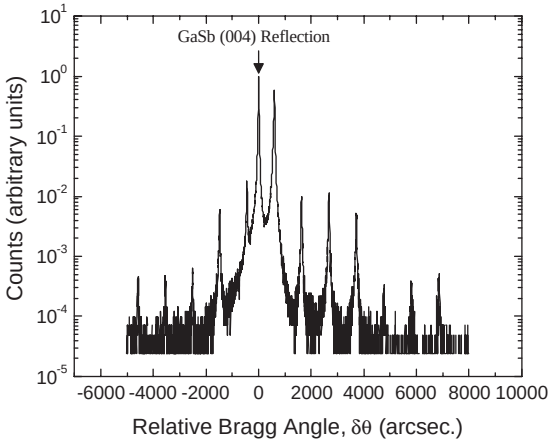

Fig. 2. X-ray rocking curve of a GaSb/InAs superlattice around the (0 0 4) GaSb reflection ($P_b = 3.4 \times 10^{-6}$).

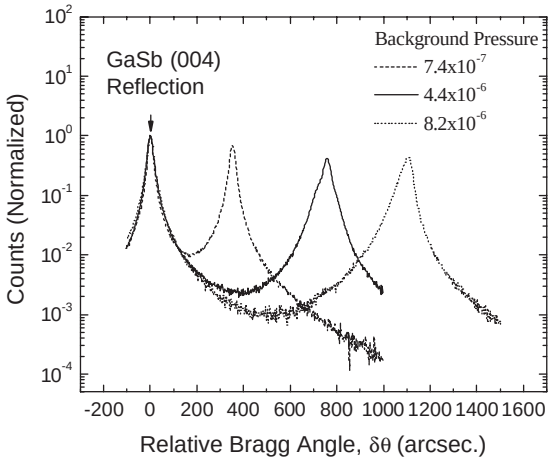

Fig. 3. Expanded view of the GaSb substrate peak and 0th order superlattice peak for several superlattices grown with varying P_b.

corresponding to an uncertainty in the strain of $\pm 1 \times 10^{-4}$. This is the limit of precision we would expect to obtain with the present technique and presumably results from variations in the substrate temperature and the As flux [8]. The strain is varied over a range of $\sim 3 \times 10^{-3}$. Larger changes in the lattice constant and total strain could presumably be achieved by adding more As with the same technique, but the SL structure investigated here begins to relax at larger strains making structural analysis difficult.

The cross-incorporation of Sb into bulk InAs and As into the bulk GaSb can be monitored directly with XSTM [2,6,9]. Fig. 5 shows an STM gray-scale image of a typical, atomically flat {1 1 0} cross-sectional surface through a GaSb/InAs superlattice grown with $P_b = 5.3 \times 10^{-6}$ Torr. In this filled state tunneling image, the "dark" (i.e. topographically lower) regions represent InAs layers and the "bright" regions the GaSb layers [5,7,10]. Note that the few brightest, cluster-like structures on the surface correspond to small, monolayer-height islands resulting from an imperfect cleave. Arsenic atoms cross-incorporated into the GaSb layers are observed as numerous dark atoms randomly distributed in the lattice. A few analogous

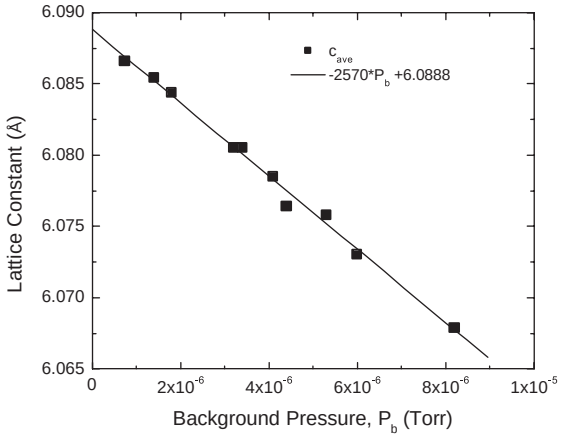

Fig. 4. The average bulk lattice constant as a function of the background pressure, P_b. The bulk value is obtained from c_z assuming Poisson's constant is 1/3. The line is a least squares fit.

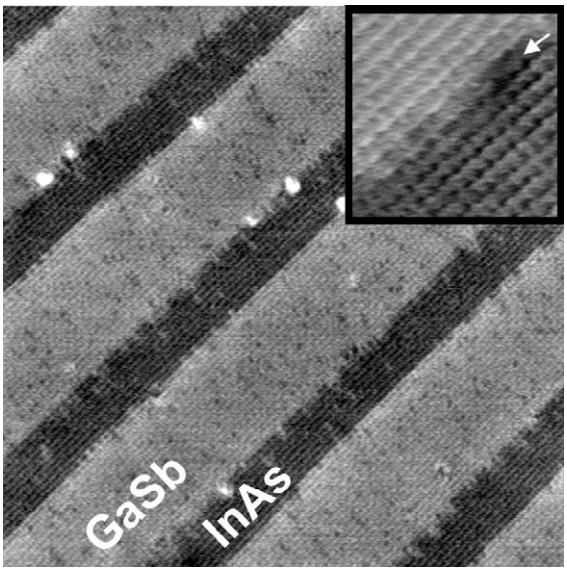

Fig. 5. XSTM image of a GaSb/InAs superlattice grown with $P_b = 5.3 \times 10^{-6}$ Torr revealing the anion sublattice (60 nm × 60 nm). Dark (bright) atoms in GaSb (InAs) layer represent As cross-incorporation (Sb cross-incorporation) Inset: Close-up (7 nm × 7 nm) of an InAs/GaSb interface where a segment of GaAs interfacial bonds are observed (dark area indicated by the arrow).

bright features are visible in the InAs, corresponding to Sb atoms that have interdiffused from the GaSb interface. Two other samples were also characterized, and the As concentrations in the GaSb layers determined by counting the cross-incorporated atoms. A similar procedure was used to determine that the Sb concentration in the InAs was about 3% in all three cases, consistent with about 0.6 ML of excess Sb on the growth surface distributed within the 20 ML of InAs [2,11]. The As cross-incorporation results are summarized in Fig. 6. For comparison, As concentrations extracted from the XRD results as described below, assuming no interface contribution, are also shown in the figure.

The difference between the XRD and XSTM results can be attributed to substitution of GaAs for InSb at the interfaces [5,6]. The average c-axis lattice constant is the sum of the contributions of the GaSb and InAs layers and the interfaces

$$c_z = \frac{(n_{\mathrm{Ga}} - \Delta) * c_{\mathrm{GaSb(As)}} + (n_{\mathrm{In}} + \Delta) * c_{\mathrm{InAs(Sb)}} + (1 - \Delta) * c_{\mathrm{InSb}} + \Delta * c_{\mathrm{GaAs}}}{n_{\mathrm{Ga}} + n_{\mathrm{In}} + 1}. \quad (2)$$

Here, $c_{\mathrm{GaSb(As)}}$, c_{InSb}, and $c_{\mathrm{InAs(Sb)}}$ are the *strained* c-axis lattice constants, c_z is the measured average c-axis lattice constant of the superlattice, Δ is the fraction of GaAs at the interface, and n_{Ga} and n_{In} are the number of monolayers of GaSb (40) and InAs (20) in the structure. Ideally, there is one half of a monolayer of InSb at each interface, i.e. $\Delta = 0$. The strain is known since the films are pseudomorphic with the GaSb substrate to a good approximation. The amount of cross-contamination—i.e. the As and Sb mole fraction in each layer—is extrapolated from the XSTM results where necessary. Then the lattice constants of $GaSb_{1-y}As_y$ and $InAs_{1-x}Sb_x$ are computed by linearly interpolating between the strained binaries (i.e. Vegard's law), and Eq. (2) is solved for Δ. The results are shown in Fig. 7. It should be noted that the derived fraction of GaAs interface bonds is an average of the two interfaces, which may not be symmetrical.

The interfaces for the growths with the lowest P_b values are about 37% GaAs-like, considerably higher than what was seen in an earlier work with a similar MEE procedure [1]. This is probably a result of higher As pressures during the interface growth. In Ref. [1], the InAs layers were grown at 0.13 ML/s versus 1 ML/s here. The lower growth rate allows In-limited InAs growth with a much lower As flux. At the GaSb-on-InAs interface, an ML of In is deposited immediately after the InAs layer while the As pressure is just starting to decline. At the InAs-on-GaSb interface, it was necessary to open the As valve ~ 1 s before the As shutter in order to obtain good morphology. This caused the As pressure to begin to build up while the In interface layer was deposited. The latter procedure was not necessary in the earlier study because the shutter alone was sufficient to control the As pressure in the Riber 32P growth chamber used there. Therefore, the As background during the In depositions at both interfaces was much higher here than in the growths described in Ref. [1].

Overall, these results suggest that almost 30% of the lattice constant decrease in these SLs comes from the change in the interface composition. Since superlattice detectors generally have much shorter periods than the superlattices examined here, the relative importance of the interface composition is expected to be

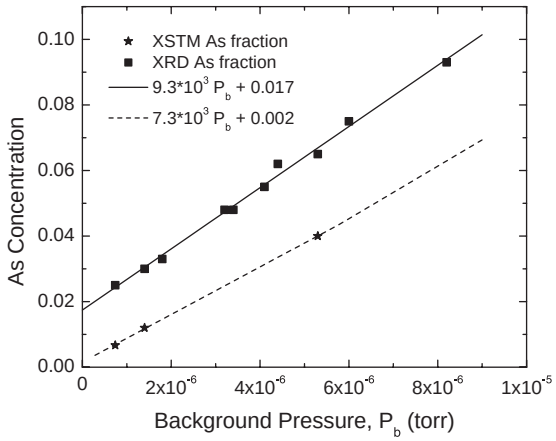

Fig. 6. As concentration vs P_b. The stars indicate concentrations determined directly by XSTM. The squares are calculated from the lattice constant assuming pure InSb interfaces and 3% Sb in the InAs layers. Smaller lattice constants imply higher As concentration. The lines are least squares fits to the data.

even greater. This expectation has been confirmed by XRD measurements of a single superlattice similar to those described here but with GaSb layers only 10 ML thick. The results are consistent if the contributions of As in the bulk and at the interfaces are both taken into account.

We can also determine an upper limit for the critical thickness of these superlattices. The resolution of the in-plane lattice constant measurement is insufficient to determine the critical thickness. However, another measure of the strain relaxation is the full- width at half-maximum (FWHM) of the 0th order superlattice X-ray peak [12]. The FWHM of this SL structure has a theoretical value of about 22 arcsec and should increase with increasing relaxation [13]. The FWHM data, shown in Fig. 8, does trend higher with increasing strain, but the minimum FWHM is $\sim$ 30 arcsec. Growth of many superlattices in our chamber indicates that this is about the minimum FWHM we can achieve, presumably because of other growth parameters such as rate non-uniformity and interface roughness. Inspection of Fig. 8 shows that this value

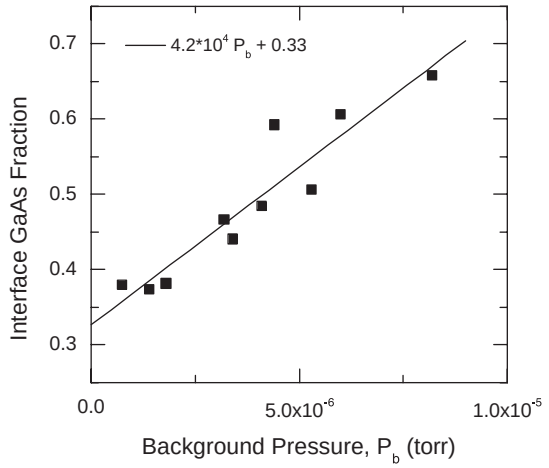

Fig. 7. The fraction of GaAs at the interfaces necessary to reconcile the XSTM data and XRD data as a function of P_b. The concentration of As in the GaSb layers has been interpolated/extrapolated from the XSTM data where necessary.

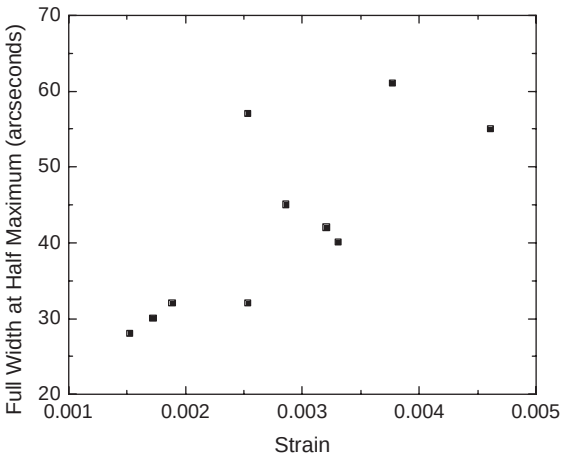

Fig. 8. Full-width at half-maximum of the 0th order superlattice X-ray peak vs. superlattice strain.

can be achieved at a strain of $\sim 2.5 \times 10^{-3}$. Below this value, the strain-induced linewidth broadening is not significant.

A similar conclusion can be drawn from Nomarski phase contrast microscopy. Under magnification, a cross-hatch pattern can be seen in relaxed samples. Cross-hatching is visible in all the samples with strain above 3×10^{-3} and one of the two samples with strain $= 2.5 \times 10^{-3}$, but not in a sample with strain equal to 1.7×10^{-3}. From this result, we again obtain an estimate for the critical strain of about $\sim 2.5 \times 10^{-3}$. These measurements must be considered an upper limit given that neither method can observe individual dislocations.

Both the InAs layers and the GaSbAs layers are well below their expected critical thicknesses. For the worst case, $GaSb_{0.92}As_{0.08}$, the equilibrium critical thickness is ~ 50 nm, about four times the layer thickness. Therefore, the observed relaxation must be attributed to the strain in the structure as a whole. In a uniform, bulk film of 900 nm thickness the critical strain is expected to be about 4×10^{-4} [14]. As is often the case, we observe relaxation only at a value several times the theoretical limit, but we cannot rule out small numbers of dislocations at lower strain values.

4. Summary

In conclusion, we have studied the cross-contamination of As in GaSb layers within InAs/GaSb superlattices. We find that the As incorporation in both the bulk of the GaSb layer and at the interfaces is linearly dependent on the As background pressure during the GaSb layer growth, and that the interfacial bonds must be taken into account to properly account for the overall lattice constant. By controlling this background pressure, the strain can be controlled over a range of at least 3×10^{-3} to within about 1×10^{-4}. The critical strain is observed to be $\leq 2.5 \times 10^{-3}$.

Acknowledgements

The Office of Naval Research supported this work. The authors thank Marc Goldenberg and Jim Culbertson for technical discussions and assistance.

References

[1] B.R. Bennett, B. Shanabrook, R.J. Wagner, J.L. Davis, J.R. Waterman, M.E. Twigg, Sol. St. Elec. 37 (1994) 733.
[2] J. Steinshnider, J. Harper, M. Weimer, C.-H. Lin, S.S. Pei, D.H. Chow, Phys. Rev. Lett. 85 (2000) 4562.
[3] J. Schmitz, J. Wagner, F. Fuchs, N. Herres, P. Koidl, J.D. Ralston, J. Crystal Growth 150 (1995) 858.
[4] J. Schmitz, J. Wagner, M. Maier, H. Obloh, P. Koidl, J.D. Ralston, Jour. Elec. Mat. 23 (1994) 1203.
[5] B.Z. Nosho, W. Barvosa-Carter, M.J. Yang, B.R. Bennett, L.J. Whitman, Surf. Sci. 465 (2000) 361.
[6] B.Z. Nosho, B.R. Bennett, L.J. Whitman, M. Goldenberg, J. Vac. Sci. Techn. B 19 (2001) 1626.
[7] S.G. Kim, S.C. Erwin, B.Z. Nosho, L.J. Whitman, Phys. Rev. B 67 (2003) 121306.
[8] S. Nemeth, B. Grietens, G. Borghs, J. Appl. Phys. 77 (1995) 3552.
[9] J. Harper, M. Weimer, C.-H. Lin, S.S. Pei, J. Vac. Sci. Techn. B 16 (1998) 1389.
[10] S.G. Kim, S. Kim, J. Shen, B.Z. Nosho, S.C. Erwin, L.J. Whitman, Int. J. Quantum Chem. 95 (2003) 561.
[11] W. Barvosa-Carter, A.S. Bracker, J.C. Culbertson, B.Z. Nosho, B.V. Shanabrook, L.J. Whitman, H. Kim, N.A. Modine, E. Kaxiras, Phys. Rev. Lett. 84 (2000) 4649.
[12] M.J. Hordon, B.L. Averbach, Acta Metall 9 (1961) 237.
[13] RADS simulation software, copyright Bede Scientific.
[14] E.A. Fitzgerald, Mat. Sci. Reports 7 (1991) 87.